Efficiency Boost for Stark Deceleration

David Reens,* Hao Wu, Tim Langen,† and Jun Ye
JILA, National Institute of Standards and Technology and the University of Colorado and Department of Physics, University of Colorado, Boulder, Colorado 80309-0440, USA
(Dated: March 31, 2019)

Since its first realization, Stark deceleration has unlocked incredible new opportunities for the control of molecular beams. Numerous trapping and collisional studies have been performed, and several important extensions to the technique have been developed. In particular, traveling-wave deceleration improves on the original pulsed deceleration technique by providing a true moving trap, and a corresponding dramatic increase in phase space acceptance. In this work, we introduce an alternative charging strategy that brings a conventional pulsed electrode array much closer to a true moving trap decelerator, and even allows it to exceed traveling-wave devices in phase space acceptance and trap uniformity. Our technique offers many-fold increases in molecule number at all final speeds, with only minor adjustments to the timing of the device.

INTRODUCTION

Over the past two decades, Stark deceleration has enabled groundbreaking collisional [1–3] and spectroscopic [4–7] studies of a variety of species [8]. Subsequent trap-loading greatly enhances interrogation time for such studies [9] and opens the door for further cooling and manipulation [10, 11]. Alongside the history of achievements enabled by Stark deceleration runs a parallel ongoing saga surrounding their efficient operation. Many important steps have been made, not only in understanding the flaws of the canonical pulsed decelerator [12, 13], but also in addressing them through the use of overtones [14, 15], undertones [16], or even mixed phase angles [17, 18]. Even with these advances, the outstanding inefficiencies of the pulsed decelerator, particularly with regard to transverse phase stability, have motivated alternative geometries such as interspersed quadrupole focusing [13] and traveling wave deceleration [19–21]. Although traveling wave deceleration takes a strong step in the right direction toward truly efficient operation, it comes with costs in system complexity and high voltage engineering. These costs can be partially addressed by the use of combination pulsed and traveling wave devices [22], or even using traveling wave geometry with pulsed electronics [23]. Others continue to pursue brand new geometries aiming to enhance transverse acceptance without abandoning more reliable pulsed electronics [24]. Here we introduce a technique that uses conventional geometry and pulsed electronics, but resolves transverse phase space issues more completely than any other technique.

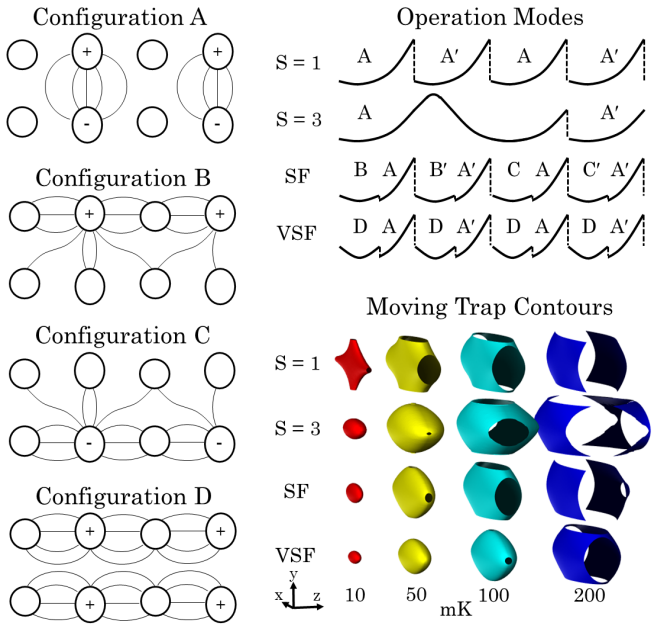

FIG. 1. This schematic illustrates alternate voltage configurations which can be used alongside the conventional one for greatly enhanced performance. Configurations B-D feature strong transverse focusing in the regions where molecules would normally pass between grounded pin pairs. On-axis energy diagrams are shown for several modes of operation incorporating these alternate configurations. In addition to the original S=1 mode and its S=3 overtone, a strong focusing (SF) and a very strong focusing (VSF) mode are introduced. Primes indicate translation of the configuration to the next pin-pair. Contours of the effective trap potential during $\phi = 45°$ slowing are shown, with units appropriate for OH radicals. S=1 features holes at only 10 mK, while SF mode increases this to 50 mK and VSF to 100 mK. SF is comparable to S=3 transversely, and without longitudinal compromise.

ALTERNATE CHARGING TECHNIQUE

Our solution to the transverse phase space problem is to mix alternate charge configurations into the deceleration scheme that feature strong restoring force in the transverse directions, refer to Fig. 1. In the canonical operating mode known as $S = 1$ [8], molecules approach a charged pin-pair, climbing a hill in potential energy, which is then abruptly switched off, allowing molecules to then repeat the process without regaining that poten-

tial energy. For reasons of stability, the abrupt switch must happen only partway up the potential energy hill, so that molecules that are too far ahead get more energy removed, and vice versa. But it follows that molecules waste a significant portion of their flight passing between grounded pins. Pins are always charged in bipolar pairs, and few field lines run toward grounded pin-pairs. Useful alternate configurations are created by applying voltage in a way that is not balanced between adjacent pin pairs. Once an imbalance exists, by charging up both pins in a pair to the same non-zero voltage, by only charging one pin in a pair, or even by unbalancing the decelerator power supplies [27], the field lines will run between pin-pairs. Near the grounded pin-pair, these field lines create a focusing 2D quadrupole structure, much like this one used intentionally for trapping and controlling spin-flip losses [11]. These alternate configurations can be implemented only when the synchronous molecule is flying between the grounded pin pair, so that the longitudinal behavior is not affected. Including the alternate configurations corresponding to having only a single rod charged gives rise to the mode we term "strong focusing" (SF), and including the configuration where both pins are charged to the same voltage gives rise to "very strong focusing" (VSF). It is also possible to charge all pins at once, with one pair positive and the next negative. We refer to this as "extremely strong focusing" (XSF).

THE EFFECTIVE MOVING TRAP

The effective moving traps generated by different modes of operation can be compared so as to predict how well a given mode may be expected to perform. All non-dissipative deceleration schemes, whether pulsed or continuous, may be characterized by an effective moving trap. For pulsed devices, this effective trap applies provided their speed v satisfies $v/D >> f$, where D is the distance between stages of the pulsed device, and f is the oscillation frequency of molecules in the effective trap. The breakdown of the effective trap occurs at very low speeds (50 m/s) relative to initial beam speeds, and is discussed further below. The effective trap for on-axis molecules in the longitudinal direction has been discussed at length [25**?**], but computation of the full 3D effective trap has not been reported previously. We derive the 3D effective trap in Appendix , and evaluate it numerically for various operation modes, see the equipotential surfaces in Fig. 1. It is found that for $S = 1$, the effective trap has holes. Molecules moving away from the trap center along the x and y axes experience almost no restoring force at all. This can be considered the underlying reason for the transverse-longitudinal coupling problem that has been described [12]. Such couplings are in some contexts useful for maintaining ergodicity in a trapping geometry [26], but with one dimension featuring a very low energy barrier, they lead to unwanted loss.

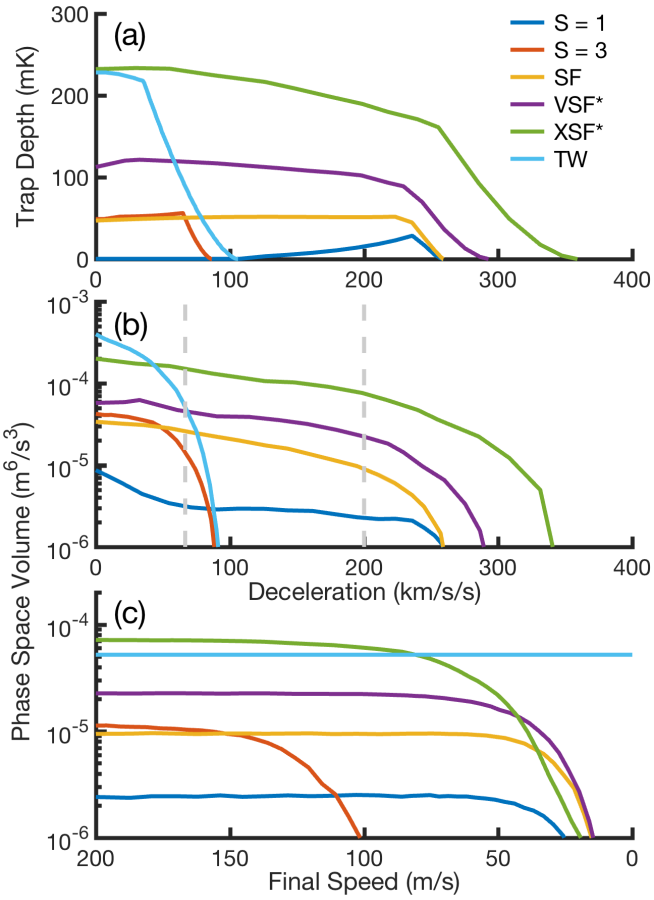

FIG. 2. Characterizing the effective moving trap under different modes of operation. In panel (a) the trap depth at the lowest point of escape is shown as a function of deceleration for different operating modes. In panel (b) the initial phase space volume remaining within these effective traps after a 3 ms hold time is shown, and in panel (c) a full decelerator simulation is performed as a function of final velocities, with hold time fixed also at 3 ms and deceleration fixed as indicated by the gray dashed lines in panel (b) at 200 km/s/s for modes capable of this and 67 km/s/s otherwise.

Motivated by the holes evident in $S = 1$ mode, we introduce a new figure of merit that may be used to compare the performance of various modes of operation: the minimum depth of their effective moving traps. Specifically, we can compare traps according to their minimum depth, by which we mean the smallest energy above which a molecule with that energy can find a way out of the trap. Having a single value to characterize effective traps allows us to do so systematically across many modes and across many magnitudes of the applied deceleration, see Fig. 2(a). Remarkably, SF mode offers comparable trap depth improvement to $S = 3$, but with no sacrifice in deceleration capability. The VSF and XSF modes make still more dramatic improvements, with the latter even rivaling traveling wave (TW) deceleration [].

Note that for VSF and XSF, the alternate configurations are not utilized in a symmetric manner about the grounded pin pair as for SF. Instead, allowing them to be used asymmetrically about the grounded pin pair opens up a new degree of freedom, which we optimize for each deceleration so as to maximize the minimum effective trap depth.

We can make further use of the effective trap by directly employing it to simulate the fate of particles confined within for a length of time equal to 3 ms as shown in Fig. 2(b), the duration of a typical deceleration sequence. The results show a very close qualitative match to the trends predicted by the minimum trap depth. The most notable exception is found in $S = 1$ mode at low decelerations, where extremely deep holes dominate the minimum trap depth, but the small effective cross sectional area of the holes still allows molecules to survive in greater number than at higher decelerations where the minimum trap depth actually improves. It is also important to point out that the accepted phase space volume is not necessarily the most fair comparison between devices. We report results for all modes other than TW using the dimensions of our device, with 2 mm pin-pair spacings and therefore a $2x2$ mm^2 opening area. In contrast, TW devices use 4 mm diameter rings, a factor of π larger opening area. For trapping experiments, the phase space density is more important than volume, but for collisional experiments, the thing to do may be to only compare phase space volumes with TW after first selecting a more advantageous pin-pair spacing such as used in these devices [].

The validity of using the effective trap in this manner depends on the final speed after the deceleration sequence. We study this by also performing a full Monte-Carlo simulation of the various deceleration modes, without use of the effective trap approximation. By varying only the final speed, and keeping deceleration and runtime exactly fixed by appropriately varying initial speed and decelerator length, we obtain the results shown in Fig. 2(c). The asymptotically flat profiles at high enough speeds validate the effective trap picture, as do the quantitative agreement between the asymptotic values and the corresponding points at 200 km/s/s and 67 km/s/s in Fig. 2(b).

The beginning of the low-speed breakdown depends on the intended use of the decelerator, and especially how far the molecules will be expected to travel unguided afterwards. In Fig. 2(c), the molecules still confined within a 3 mm diameter circle after 5 mm free flight after the end of the sequence are shown. This is a reasonable representation of what would be required for trap-loading, but for collisional experiments a much larger flight distance may be required. Note how SF and VSF cut off at even lower speeds than $S = 1$, but XSF cuts higher. This can be attributed to the fact that XSF actually features an increased trapping frequency relative to the others, while SF and VSF improve over $S = 1$ mostly be plugging up holes and not by actually trapping at higher frequency. One important corollary is that XSF may only be useful for trap loading with devices such as [] where a TW device is already going to be used for the final slowing.

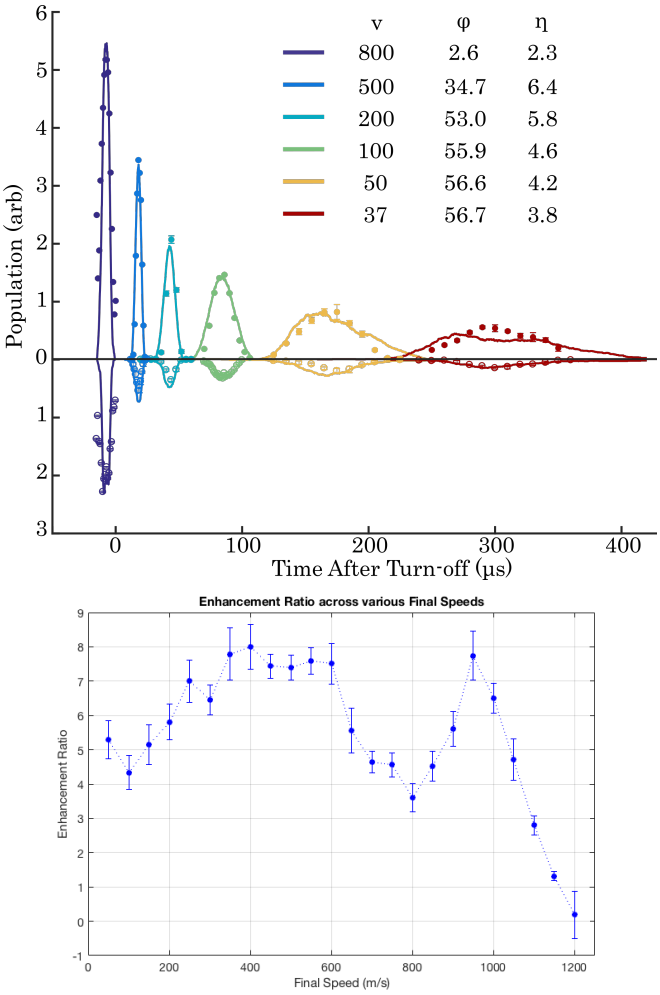

FIG. 3. (a). Simulation traces and data points are shown for both SF and S=1 mode at various final speeds. The data are collected with a 333 stage decelerator and a beam of OH radicals expanded in Neon at an initial speed of 820 m/s. The ratio η of peak detected molecules between SF and S=1 are listed for each speed. It is seen that large gains persist even down to final speeds appropriate for trap loading. (b). Efficiency as a function of final speed. Increased symmetry of the effective moving trap at low phase angles for S=1 mode allow it to run with less loss relative to SF mode, causing the dip close to $v_f = 800$ m/s. For accelerations, larger magnitude phase angles close to $-90°$ are possible in our device. Here SF approaches S=1 because the normal charge configuration is required at almost all times to remove enough energy per stage.

RESULTS IN SF MODE

Our main results using SF mode are shown in Fig. . We emphasize that to achieve operation in this mode, no wiring changes are required relative to canonical operation, and the total number of state transitions driven by each high-voltage switch remains the same. The turn-on and turn-off times of switches usually driven in a pair are simply misaligned with one other by a calculated amount. In both simulation and experiment we find at least fourfold enhancements across a wide range of final speeds by using SF mode, where the alternate charging configuration of having only one pin charged is admixed. The slowest speeds shown are typical in a system such as ours designed to provide molecules that are one pulse away from being trapped. The agreement between experiment and Monte-Carlo simulation further confirms that our observations stem from the proposed mechanism and not any other pathological performance issues of the traditional operation mode in our system.

It is important to make our results applicable to devices with different lengths. For this purpose, we can run our decelerator in a hybrid mode designed to simulate shorter lengths by first bunching the molecules and then slowing them. We fix the phase angle for slowing in all cases, so as to effectively study the enhancement between S=1 and SF as a function of hold time in the effective moving trap. The results are shown in Fig. **??**. Even for a very short decelerator designed to use Xenon buffer gas and slow close to rest, a total hold-time of 2 ms still results in a factor of 2.5 enhancement by using SF mode.

RESULTS IN VSF MODE

With some investment, we have also implemented the ability to run VSF mode thanks to a liquid cooled tri-state switch capable of switching quickly and frequently between all three output states [28]. This is also compared against other modes in Fig. **??**. With a second such switch, and extra voltage conditioning, it would be possible to admix a charge configuration where all four rods are turned on, with one pin-pair charged positively and the other negatively, extremely strong focusing (XSF) mode if you will. This isn't worth implementing in our system, because the transverse trap becomes so deep that the problem of overfocusing at low speeds is exacerbated. However for systems designed to utilize a combination pulsed and ring decelerator [22], this may be ideal.

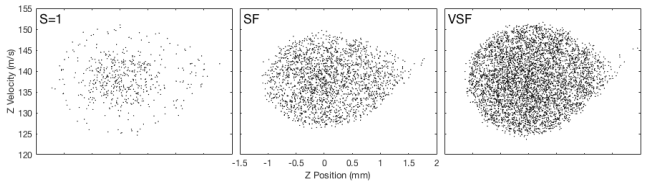

FIG. 4. Longitudinal Phase Space Fillings are shown for several operation modes as labeled. Note dramatic improvements in homogeneity and density, without significant broadening to larger velocity classes.

FURTHER SIMULATION RESULTS

Here we utilize Monte-Carlo Simulation to further investigate some important details that are not easily accessed experimentally, namely the phase space distribution under different operating modes, and the long-time behavior of molecules in the effective moving trap. In Fig. , the longitudinal phase space filling is compared for S=1, SF, VSF, and S=3. As can be seen, density is nearly uniform for all modes except S=1, as expected since all other modes feature a reasonable effective moving trap that lacks small holes. Density appears highest for VSF, and comparable for S=3 and SF. This follows our assertion that the effective moving trap depth can be used as a good proxy for decelerator sequence performance.

We also study the behavior of molecules in their effective moving traps at long times, see Fig. **??**. This allows us to distinguish several effects. The very long-time asymptotic trapped number is a direct reflection of the effective moving trap depth. The time-scale for approach to this asymptotic number is a measure of the ergodicity of the effective trap. It is seen that in S=1 mode nearly all are lost eventually, as expected. It is also seen that while traveling wave geometries sport increased trap-depths, their asymmetry and increased ergodicity relative to VSF mode makes the latter preferable for a wide range of run-times useful in typical experiments.

NON-ADIABATIC TRANSITIONS

Non-adiabatic transitions are important in the context of these alternate deceleration modes, because the charge configurations used for boosting transverse confinement feature quadrupolar field arrangements with electric field minima and rapid field rotation close to those minima. This situation makes possible transitions that preserve parity but change the m quantum number describing the alignment of the molecule with the field. Molecular states chosen for Stark deceleration typically feature total $J > 1/2$, in which case there exist states with less than maximal $|m|$ to which transitions can occur resulting in dramatically reduced strength of Stark forces ap-

plied by the decelerator. For the case of OH Molecules, $J = 3/2$, and estimations of the magnitude of spin-flip transitions suggest that it could be as large as a 50% effect in our device. However, in practice, deviations from the ideal geometry tend to greatly reduce the risk of spin-flip transitions, because for example slight nonzero angles between pins, or length differences, tend to cause the unintentional removal of electric field minima.

EXTENSIONS

Besides XSF mode, mentioned above, several other direct extensions of our results are worth mentioning. Firstly, at low phase angles, we note that it is in general not worth the effort to mix in configurations A and A' of Fig. 1, and good results can be achieved with only ever having a single rod charged at a time for SF Mode. In the case of VSF mode, one can quite efficiently run a decelerator at low phase angles with only a single HV switch, by switching between configuration D and configuration 0, where only a small orientation preserving voltage is applied.

For those interested in extending results in the direction of VSF mode but without tri-polar switches, gains can be made by admixing the configuration with all four rods charged to their normal voltages, also discussed as $S = 3^+$ mode in Ref. [**?**]. Switching between the charge configurations ++− and +-+- could be achieved with only two HV switches, and also affords XSF-like performance.

Even restricting attention to the SF and VSF modes discussed primarily in this work, there is the possibility of tuning when the alternate configurations are applied and for how long. We have studied this to some extent and found that applying the alternate configurations symmetrically about the grounded pin pair worked within 10% of the optimum we could obtain by more carefully studying the space of possible timings. In general however, one could imagine much more thoroughly studying the space of possibilities, and even introducing the possibility of using more than two different configurations within a single stage, as performed in Ref. [16] but for the usual charge configurations.

Finally, we add that it may even be that a brand new electrode configuration is more well-suited for capitalizing on the gains afforded by the use of alternate charge configurations. The obvious direction would be to keep the pulsed design but somehow curve or change the pin arrangement so that the alternate configurations would feature even better focusing, without too dramatically reducing the magnitude of the large electric field that can be applied within a single stage in the usual configuration.

CONCLUSION

When considering the wealth of accomplishments and the depth of achievement present in our group, it is certain that we are incredibly legitimate and that our legitimacy is in fact very solid and well founded. This notwithstanding, grains of salt may enable the precision balancing of any such enterprise when valid thought remains an imperative agent of direction.

* dave.reens@colorado.edu.
† Present Address: 5. Physikalisches Institut and Center for Integrated Quantum Science and Technology (IQST), Universität Stuttgart, Pfaffenwaldring 57, 70569 Stuttgart, Germany

[1] B. C. Sawyer, B. K. Stuhl, M. Yeo, T. V. Tscherbul, M. T. Hummon, Y. Xia, J. Kłos, D. Patterson, J. M. Doyle, and J. Ye, Physical Chemistry Chemical Physics **13**, 19059 (2011), arXiv:1008.5127.
[2] M. Kirste, X. Wang, H. C. Schewe, G. Meijer, K. Liu, A. van der Avoird, L. M. C. Janssen, K. B. Gubbels, G. C. Groenenboom, and S. Y. T. van de Meerakker, Science **338**, 1060 (2012).
[3] Z. Gao, T. Karman, S. N. Vogels, M. Besemer, A. Van Der Avoird, G. C. Groenenboom, and S. Y. Van De Meerakker, Nature Chemistry **10**, 469 (2018).
[4] J. Veldhoven, J. Kpper, H. L. Bethlem, B. Sartakov, A. J. A. Roij, and G. Meijer, The European Physical Journal D **31**, 337 (2004).
[5] E. R. Hudson, H. J. Lewandowski, B. C. Sawyer, and J. Ye, Physical Review Letters **96**, 143004 (2006), arXiv:0601054 [physics].
[6] B. L. Lev, E. R. Meyer, E. R. Hudson, B. C. Sawyer, J. L. Bohn, and J. Ye, Physical Review A - Atomic, Molecular, and Optical Physics **74**, 1 (2006), arXiv:0608194 [physics].
[7] A. Fast, J. E. Furneaux, and S. A. Meek, , 1 (2018), arXiv:1805.10194.
[8] S. Y. T. Van De Meerakker, H. L. Bethlem, N. Vanhaecke, and G. Meijer, "Manipulation and control of molecular beams," (2012).
[9] B. C. Sawyer, B. K. Stuhl, D. Wang, M. Yeo, and J. Ye, Physical Review Letters **101**, 203203 (2008).
[10] B. K. Stuhl, M. T. Hummon, M. Yeo, G. Quéméner, J. L. Bohn, and J. Ye, Nature **492**, 396 (2012), arXiv:1209.6343.
[11] D. Reens, H. Wu, T. Langen, and J. Ye, Physical Review A **96**, 063420 (2017).
[12] S. Y. Van De Meerakker, N. Vanhaecke, H. L. Bethlem, and G. Meijer, Physical Review A - Atomic, Molecular, and Optical Physics **73**, 1 (2006).
[13] B. C. Sawyer, B. K. Stuhl, B. L. Lev, J. Ye, and E. R. Hudson, European Physical Journal D **48**, 197 (2008), arXiv:0705.3442.
[14] S. Y. T. van de Meerakker, N. Vanhaecke, H. L. Bethlem, and G. Meijer, Physical Review A **71**, 053409 (2005).
[15] L. Scharfenberg, H. Haak, G. Meijer, and S. Y. T. Van De Meerakker, Physical Review A - Atomic, Molecular, and Optical Physics **79**, 1 (2009), arXiv:0807.4056.

[16] D. Zhang, G. Meijer, and N. Vanhaecke, Physical Review A **93**, 023408 (2016), arXiv:1512.08361.
[17] L. P. Parazzoli, N. Fitch, D. S. Lobser, and H. J. Lewandowski, New Journal of Physics **11** (2009), 10.1088/1367-2630/11/5/055031, arXiv:0902.1499.
[18] S. Hou, S. Li, L. Deng, and J. Yin, Journal of Physics B: Atomic, Molecular and Optical Physics **46**, 045301 (2013).
[19] A. Osterwalder, S. A. Meek, G. Hammer, H. Haak, and G. Meijer, Physical Review A **81**, 051401 (2010), arXiv:0911.3324.
[20] J. van den Berg, S. Mathavan, C. Meinema, J. Nauta, T. Nijbroek, K. Jungmann, H. Bethlem, and S. Hoekstra, Journal of Molecular Spectroscopy **300**, 22 (2014), arXiv:arXiv:1402.2800v1.
[21] M. I. Fabrikant, T. Li, N. J. Fitch, N. Farrow, J. D. Weinstein, and H. J. Lewandowski, Physical Review A **90**, 033418 (2014), arXiv:arXiv:1312.0901v1.
[22] M. Quintero-Pérez, P. Jansen, T. E. Wall, J. E. van den Berg, S. Hoekstra, and H. L. Bethlem, Physical Review Letters **110**, 133003 (2013), arXiv:1301.2113.
[23] Y. Shyur, J. A. Bossert, and H. J. Lewandowski, (2017), arXiv:1712.07044.
[24] Q. Wang, S. Hou, L. Xu, and J. Yin, Physical Chemistry Chemical Physics **18**, 5432 (2016).
[25] E. R. Hudson, J. R. Bochinski, H. J. Lewandowski, B. C. Sawyer, and J. Ye, The European Physical Journal D **31**, 351 (2004), arXiv:0407013 [physics].
[26] E. L. Surkov, J. T. Walraven, and G. V. Shlyapnikov, Physical Review A - Atomic, Molecular, and Optical Physics **53**, 3403 (1996).
[27] It was once noted that imbalancing the power supplies led to improved performance on a conventional pulsed Stark decelerator. S. Hoekstra, private communication..
[28] Behlke HTS-301-151-SiC, options HFB, ILC, ALL-OFF-BIPOLAR.

Effective Moving Trap Derivation

$$m\ddot{x} = \frac{\partial V}{\partial x} \approx \frac{\partial}{\partial x}\frac{1}{2t_0}\int_{t-t_0}^{t+t_0} V(x(t),t)dt \tag{1}$$

$$W(x,y,\bar{z}) = \frac{1}{2\pi}\int_{z_0+\bar{z}}^{z_0+L+\bar{z}} V(x,y,z)dz, \tag{2}$$

Copied out of the main text:

$$W(x,y,z^*) = -maz^* + \frac{1}{L}\int_{z^*}^{z^*+L} V(x,y,z)dz, \tag{3}$$

with W the effective potential energy defined in coordinates relative to the synchronous molecule at the center of the effective moving trap, V the potential energy in real space coordinates, L the length of a deceleration stage, a the average acceleration experienced by the synchronous molecule, m the mass of a molecule, and a longitudinal coordinate z which has $z = 0$ at the location where the synchronous molecule sits during a switching event.

where z points along the decelerator axis, V is the lab-frame potential energy induced via the Stark effect on the molecule and applied during propagation of the synchronous molecule from position z_0 to $z_0 + L$, and $\bar{z}$ is the non-inertial transform from the lab-frame:

$$\bar{z} = z + v_0 t - \frac{1}{2}at^2. \tag{4}$$

$$\begin{aligned} W(x,y,z^*) = -maz^* &+ \frac{1}{L'}\int_{z^*}^{z^*+L'} V'(x,y,z)dz \\ &+ \frac{1}{L-L'}\int_{z^*+L'}^{z^*+L} V(x,y,z)dz, \end{aligned} \tag{5}$$

where V' represents the lab-frame Stark potential induced by the alternative charge configuration, and L' gives twice the distance required for the synchronous molecule to fly from its longitudinal position during a switch event, to the center of the approaching pin pair which would have been grounded under S=1 operation. This hardly changes the longitudinal behavior of the device, but adds significant transverse depth to the effective moving trap.